

## Normal-Mode Spectroscopy of a Single-Bound-Atom-Cavity System

P. Maunz, T. Puppe, I. Schuster, N. Syassen, P. W. H. Pinkse, and G. Rempe

*Max-Planck-Institut für Quantenoptik, Hans-Kopfermann-Strasse 1, D-85748 Garching, Germany*

(Received 18 June 2004; published 27 January 2005)

The energy-level structure of a single atom strongly coupled to the mode of a high-finesse optical cavity is investigated. The atom is stored in an intracavity dipole trap and cavity cooling is used to compensate for inevitable heating. Two well-resolved normal modes are observed both in the cavity transmission and the trap lifetime. The experiment is in good agreement with a Monte Carlo simulation, demonstrating our ability to localize the atom to within  $\lambda/10$  at a cavity antinode.

DOI: 10.1103/PhysRevLett.94.033002

PACS numbers: 32.80.Pj, 42.50.-p

Experimental research in quantum information science with atoms and ions [1] is based on the ability to control individual particles in a truly deterministic manner. While spectacular advances have recently been achieved with trapped ions interacting via phonons [2,3], the precise control of the motion of atoms exchanging photons inside an optical cavity [4] or emitting single photons on demand [5,6] is still a challenge. Although very successful, experiments in cavity quantum electrodynamics with single laser-cooled atoms [7–9] are complicated by the motion of the atom in the standing-wave mode of the optical cavity [10,11]. The lack of control over the atomic motion is mainly due to the heating effects of the various laser fields employed to trap and excite the atom inside the cavity in combination with the limited ability to cool the atom between two highly reflecting mirrors facing each other at a microscopic distance [12,13]. Only recently, good localization of the atom at an antinode of the cavity mode has been achieved by applying optical molasses [14] or a novel cavity cooling force [15] to a trapped atom.

In this Letter, we go one step further and employ cavity cooling to probe the energy spectrum of a single trapped atom strongly coupled to a high-finesse resonator [16,17]. In previous experiments using thermal beams, the spectrum was explored only for many atoms [18,19], one atom on average [20,21], or single cold atoms transiting the cavity [22]. Our experiment is the first in which the normal-mode (or vacuum-Rabi) splitting of a single atom trapped inside a cavity is observed. Both the cavity transmission and the trapping time are investigated. The results agree with a Monte Carlo simulation and demonstrate that remarkably good control can be obtained over this fundamental quantum system.

The cavity used in the experiment (Fig. 1) has a finesse  $\mathcal{F} = 4.4 \times 10^5$ , a mode waist  $w_0 = 29 \mu\text{m}$ , and a length  $l = 122 \mu\text{m}$  [15]. A single  $\text{TEM}_{00}$  mode of the cavity is near resonant with the  $5^2S_{1/2}F = 3, m_F = 3 \leftrightarrow 5^2P_{3/2}F = 4, m_F = 4$  transition of  $^{85}\text{Rb}$  at  $\lambda = 780.2 \text{ nm}$ . The atom-cavity coupling at an antinode of the standing wave,  $g/2\pi = 16 \text{ MHz}$ , is large compared to the amplitude decay rates of the atomic excitation,  $\gamma/2\pi = 3 \text{ MHz}$ ,

and the cavity field,  $\kappa/2\pi = 1.4 \text{ MHz}$ . Strong coupling is reached, resulting in critical photon and atom numbers  $n_0 = \gamma^2/2g^2 \approx 1/60$  and  $N_0 = 2\gamma\kappa/g^2 \approx 1/30$ , respectively. This strongly coupled atom-cavity system is probed by a weak near-resonant beam impinging on the cavity. The probe beam is also used to cool the axial motion of the atom. A second  $\text{TEM}_{00}$  mode supported by the cavity, two free spectral ranges red detuned with respect to the near-resonant mode, is used to trap the atom in the cavity. This mode is resonantly excited by a trap laser at  $785.3 \text{ nm}$ . The far-detuned light is generated by a grating- and current-stabilized laser diode and has a linewidth of about  $20 \text{ kHz}$  rms. The cavity length is continuously stabilized to this trap laser. The two light fields transmitted through the cavity are separated by a holographic grating. The trap light is directed to a photomultiplier, whereas the probe light is further filtered by a narrow-band interference filter and then detected by two single-photon counting modules. The setup achieves a quantum efficiency of 32% for the probe light transmitted through the cavity and a suppression of the trap light on the photon counting modules of more than 70 dB.

Laser-cooled  $^{85}\text{Rb}$  atoms are injected from below by means of an atomic fountain [8]. The parameters of the fountain are chosen to get well-separated signals of single atoms which have a velocity below  $10 \text{ cm/s}$ . The atoms are guided into the antinodes of the far-detuned field by a weak dipole potential with a trap depth of  $400 \mu\text{K}$ . The near-resonant light used to detect the atom is blue detuned with

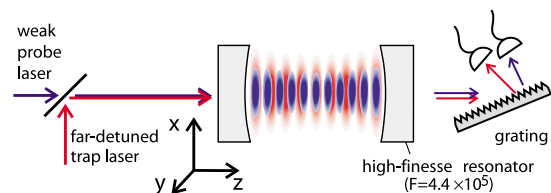


FIG. 1 (color online). Experimental setup: The high-finesse cavity is excited by a weak near-resonant probe field and a strong far-red-detuned trap field.  $^{85}\text{Rb}$  atoms are injected from below. Behind the cavity, the two light fields are separated by a grating and measured with independent photodetectors.

respect to the atomic resonance,  $\Delta_a = \omega_p - \omega_a = 2\pi \times 35$  MHz, and resonant with the cavity,  $\Delta_c = \omega_p - \omega_c = 0$ . The presence of the atom inside the cavity tunes the atom-cavity system out of resonance with the probe laser. The resulting dramatic drop of the transmission allows the detection of an atom with a high signal-to-noise ratio and a high bandwidth. Since the atoms are guided into the antinodes of the far-detuned field, only atoms which enter near the cavity center, where the antinodes of the two light fields coincide, are strongly coupled to the probe beam and cause a deep drop of the transmission. Upon detection of a strongly coupled atom in the cavity, the trap depth of the conservative dipole potential is increased to values between 1.3 and 1.9 mK. This compensates for the kinetic energy of the atom and leads to trapping. It is noteworthy that all atoms which activated the trigger are captured in the trap. We estimate the probability to trap more than one atom at a time to be below 0.4%.

The storage time of a single atom in the far-detuned dipole trap without any near-resonant light is about 30 ms as described in Ref. [15]. The storage time is limited by axial parametric heating due to intensity fluctuations of the intracavity dipole trap. The dipole force of the probe light, which caused a shift and a distortion of the measured spectra in earlier experiments [4,22], can be neglected because it is much weaker than the dipole force of the far-detuned light. However, depending on the relative frequencies of the atomic transition, cavity resonance, and probe laser, nonconservative forces can heat or cool the atom [23–25] mainly along the cavity axis. In order to measure the atom-cavity spectrum, it is necessary to probe the system at detunings for which these forces lead to strong heating. This quickly reduces the atomic localization, and severely limits the available probe time by boiling the atom out of the trap. To compensate the disastrous effect of heating, cooling intervals are applied to reestablish strong coupling of the atom to the cavity. This can be achieved by switching the probe laser to parameters for which the velocity-dependent forces lead to efficient cooling [15]. Of course, in the radial direction, the atom is heated by scattering photons of the near-resonant probe light. Since there is no radial cooling mechanism, this heating mechanism contributes to the experimentally observed loss rate of atoms from the trap.

These considerations lead to the following protocol to perform the atom-cavity spectroscopy: After capturing the atom in the trap, a 500  $\mu$ s long cooling interval is used to improve the localization of the atom and to determine its coupling strength by monitoring the cavity transmission with a resonant probe laser ( $\Delta_c = 0$ ). This is followed by a 100  $\mu$ s long probe interval, where the frequency of the probe laser is changed to an adjustable but fixed value  $\Delta_c$ . This sequence of cooling and probing intervals is then repeated. As long as the atom is stored in the trap, the transmission during the cooling intervals is low, while it is

high if the atom has left. The end of the last cooling interval during which the transmission is below 80% of the empty-cavity transmission determines the exit time of the atom. Within this sequence, each probe interval is enclosed by two cooling intervals in which the coupling strength before and after the probe interval can be determined independently of the probing. This allows the exclusion of probe intervals during which the atom is only weakly coupled to the cavity mode. We find that in about 25% of the probe intervals in which an atom resides in the trap, both cooling intervals have a transmission below 2% of that of the empty cavity. These probe intervals are defined as “strongly coupled” and are used for further analysis. The whole protocol is repeated for different atoms and different values of  $\Delta_c$ .

Figure 2 shows the average cavity transmission during the strongly coupled probe intervals as a function of the probe detuning. The four spectra are obtained for different atom-cavity detunings and all show two well-resolved normal modes. Together, they display the avoided crossing between the atomic and the cavity resonances [26]. The atom-cavity detuning is adjusted by tuning the atomic

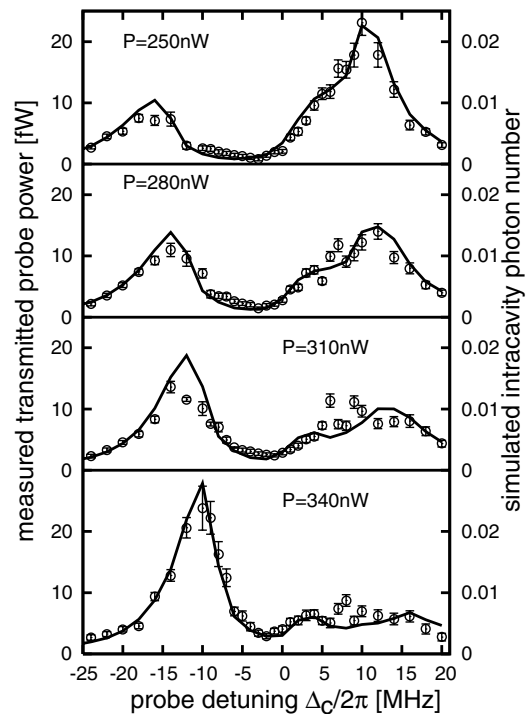


FIG. 2. Transmission of the cavity containing a single trapped and strongly coupled atom (circles). The detuning between the cavity and the atom is adjusted by tuning the Stark shift of the atom via the trapping-field power expressed in terms of the transmitted power,  $P$ . The average transmission during probe intervals for which the atom is found to be strongly coupled by independent qualification (see text) shows well-resolved normal-mode peaks. On average each point includes the data from about 350 probe intervals collected from between 35 and 1000 atoms. A Monte Carlo simulation (solid lines) describes the data well.

resonance via the dynamic Stark effect induced by the far-detuned trap light. The induced (position-dependent) shift,  $\Delta_S$ , of the atomic resonance frequency is proportional to the trap depth. For a transmitted power of the trap light of about 280 nW the dynamic Stark shift compensates the initial atom-cavity detuning of  $2\pi \times 35$  MHz. The eigenstates of the atom-cavity system (dressed states) are superpositions of the atomic ground state together with a cavity photon and the atomic excited state without a cavity photon. Since the probe laser excites only the cavity mode, the excitation of a dressed state is proportional to the contribution of the cavity state to the dressed state. This contribution depends on the atom-cavity detuning and explains the observation that the height of the left normal-mode peak increases with increasing Stark shift, while that of the right peak decreases. For zero detuning between atom and cavity (about  $P = 280$  nW), the contributions from the atomic and the cavity states are equal so that the normal modes have the same height and reach a minimum splitting of  $2g$ . Here, the observed splitting of about  $2 \times 2\pi \times 12$  MHz is only slightly smaller than the maximal possible splitting of  $2 \times 2\pi \times 16$  MHz expected for a pointlike atom at rest at an antinode. This proves that the atom is localized in the regime of strong coupling with  $g \gg (\gamma, \kappa)$ .

For a stationary atom, the widths of the two normal modes are given by a weighted mean of the atomic and cavity linewidths. However, since the atom is not fixed at an antinode of the probe field, but oscillates in the trap, the atom-cavity coupling is time dependent. This leads to fluctuating frequencies of the normal modes, and therefore the measured spectra are broadened.

The different widths of the normal modes of the spectra in Fig. 2 can be explained by taking into account the position-dependent Stark shift for a moving atom: An atom close to an antinode of the trapping field experiences a larger Stark shift, which shifts both normal modes to larger probe detunings. Near the center of the cavity, where the antinodes of both light fields overlap, this atom is also close to an antinode of the probe field. Therefore its coupling to the cavity is also larger. This increases the splitting of the normal modes. Consequently, the frequency of the left normal mode is only weakly dependent on the atomic position while the two effects add up for the right normal mode. This broadens the right peak to a greater extent than the left.

The exact width and line shape of the measured normal modes are influenced by the details of the atomic motion in the trap. Cavity heating and cooling strongly depend on the atomic position and the frequency of the probe laser. These forces determine the atomic motion in a complex way. In order to obtain more information on the atomic motion we compare the measured spectra with the results of a Monte Carlo simulation. Here a pointlike atom is propagated in space according to a stochastic differential equation for the atomic position and momen-

tum. The forces and momentum diffusion are given by analytic equations for the combined atom-cavity-trap system. Parametric heating by the dipole trap is implemented by a randomly changing potential depth. To model the experiment in detail, single atoms are injected at random positions into the mode. Upon activating the trigger, the trap depth of the trapping field is increased, and the atom is exposed to the alternating cooling and probing scheme. The atomic trajectory is recorded until the atom leaves the cavity. The simulated transmission is evaluated in the same way as the experimental data.

Results are also shown in Fig. 2 and agree well with the experimental data if the power of the trapping field is reduced by 30% with respect to the intracavity power determined from the measured cavity transmission. This discrepancy could be explained by different transmissions of the two cavity mirrors. For consistency, the probe light power in the simulation is reduced by the same amount. The simulation also allows one to calculate the spatial probability distribution of the atom in the trap. The axial distribution has a width (FWHM) of  $\lambda/7$  if all probe intervals are included. If only strongly coupled probe intervals (as defined above) are considered, the atom is axially confined to a width of  $\lambda/10$  around the antinodes of the dipole trap. The probability distribution of the simulated atom-cavity coupling (in three dimensions) is shown in Fig. 3. It shows that our selection scheme eliminates the occurrence of probe intervals with weak atom-cavity coupling and an average coupling of about  $2\pi \times 13$  MHz is reached. This agrees well with the experimentally achieved coupling of  $2\pi \times 12$  MHz.

Further characterization of the normal modes can be obtained by investigating the average storage time of the atom in the trap as a function of the detuning during the probe intervals. While the atom is probed, additional heating can lead to a loss of the atom from the trap. The probe-induced loss rate is shown in Fig. 4. These spectra also

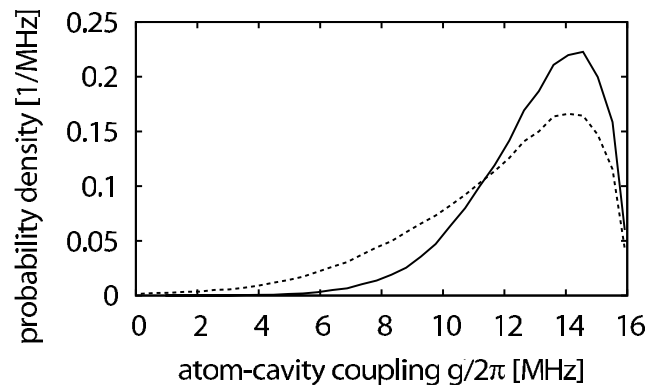


FIG. 3. Simulated probability distribution of the atom-cavity coupling for all probe intervals (dotted line) and for the strongly coupled intervals (solid line). Qualification completely eliminates the occurrence of probe intervals with weak coupling,  $g \lesssim (\gamma, \kappa)$ .

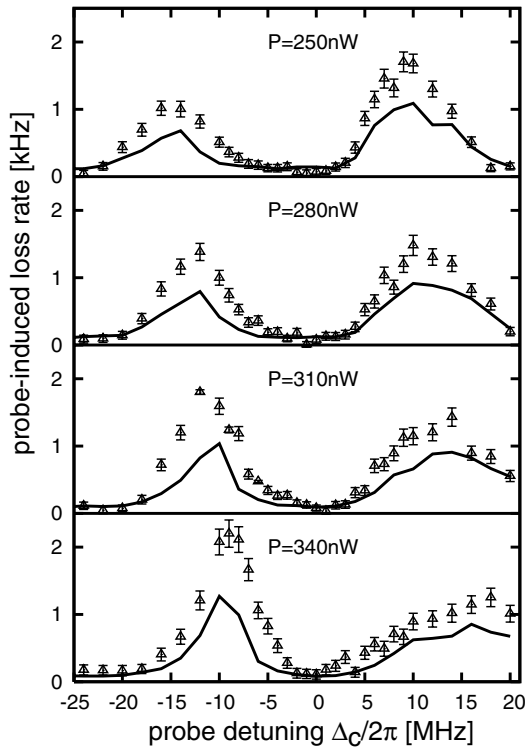


FIG. 4. Probe-induced loss rate of atoms from the trap (triangles) for different detunings between cavity and atom, adjusted by varying the trapping-field power. No qualification is employed. The experiment is in qualitative agreement with a Monte Carlo simulation (solid lines): the observed frequencies, widths, and relative heights of the normal-mode peaks are well described by the simulation. Only the absolute value of the measured rate exceeds that of the simulation. This could be explained by fluctuations of experimental parameters not taken into account in the simulation, e.g., the lack of shot noise in the modeling of atom capture. For all probe detunings the simulated atomic excitation is below 1.4%.

show two well-resolved peaks at detunings for which the excitation of the system is high. The measurements are in qualitative agreement with our Monte Carlo simulation. The simulation shows that for zero and large probe detunings, spontaneous emission accounts for about 75% of the probe-induced loss rate. On the normal-mode resonances, momentum diffusion caused by dipole-force fluctuations of the probe light generates additional heating, which causes more than 80% of the probe-induced loss rate. This makes the normal modes clearly visible in the probe-induced loss rate.

In conclusion, cavity cooling has been applied to reliably localize a single trapped atom in the strong-coupling region of a high-finesse cavity. Two well-resolved normal modes are observed both in cavity transmission and the

atomic loss rate from the trap. The ability to individually excite the normal modes of a bound atom-cavity system opens up a wealth of new possibilities including the realization of a quantum-logic gate [27] or the control of the propagation of a light pulse [28] with exactly one atom.

- 
- [1] C. Monroe, *Nature (London)* **416**, 238 (2002).
  - [2] M. Riebe *et al.*, *Nature (London)* **429**, 734 (2004).
  - [3] M. D. Barrett *et al.*, *Nature (London)* **429**, 737 (2004).
  - [4] P. Münstermann, T. Fischer, P. Maunz, P. W. H. Pinkse, and G. Rempe, *Phys. Rev. Lett.* **84**, 4068 (2000).
  - [5] A. Kuhn, M. Hennrich, and G. Rempe, *Phys. Rev. Lett.* **89**, 067901 (2002).
  - [6] J. McKeever *et al.*, *Science* **303**, 1992 (2004).
  - [7] H. Mabuchi, Q. A. Turchette, M. S. Chapman, and H. J. Kimble, *Opt. Lett.* **21**, 1393 (1996).
  - [8] P. Münstermann, T. Fischer, P. W. H. Pinkse, and G. Rempe, *Opt. Commun.* **159**, 63 (1999).
  - [9] J. A. Sauer, K. M. Fortier, M. S. Chang, C. D. Hamley, and M. S. Chapman, *Phys. Rev. A* **69**, 051804(R) (2004).
  - [10] P. W. H. Pinkse, T. Fischer, P. Maunz, and G. Rempe, *Nature (London)* **404**, 365 (2000).
  - [11] C. J. Hood, T. W. Lynn, A. C. Doherty, A. S. Parkins, and H. J. Kimble, *Science* **287**, 1447 (2000).
  - [12] J. Ye, D. W. Vernooy, and H. J. Kimble, *Phys. Rev. Lett.* **83**, 4987 (1999).
  - [13] T. Fischer, P. Maunz, P. W. H. Pinkse, T. Puppe, and G. Rempe, *Phys. Rev. Lett.* **88**, 163002 (2002).
  - [14] J. McKeever *et al.*, *Phys. Rev. Lett.* **90**, 133602 (2003).
  - [15] P. Maunz *et al.*, *Nature (London)* **428**, 50 (2004).
  - [16] J. J. Sanchez-Mondragon, N. B. Narozhny, and J. H. Eberly, *Phys. Rev. Lett.* **51**, 550 (1983); **51**, 1925(E) (1983).
  - [17] G. S. Agarwal, *Phys. Rev. Lett.* **53**, 1732 (1984).
  - [18] Y. Zhu *et al.*, *Phys. Rev. Lett.* **64**, 2499 (1990).
  - [19] J. Gripp, S. L. Mielke, and L. A. Orozco, *Phys. Rev. A* **56**, 3262 (1997).
  - [20] R. J. Thompson, G. Rempe, and H. J. Kimble, *Phys. Rev. Lett.* **68**, 1132 (1992).
  - [21] J. J. Childs, K. An, M. S. Otteson, R. R. Dasari, and M. S. Feld, *Phys. Rev. Lett.* **77**, 2901 (1996).
  - [22] C. J. Hood, M. S. Chapman, T. W. Lynn, and H. J. Kimble, *Phys. Rev. Lett.* **80**, 4157 (1998).
  - [23] G. Hechenblaikner, M. Gangl, P. Horak, and H. Ritsch, *Phys. Rev. A* **58**, 3030 (1998).
  - [24] P. Münstermann, T. Fischer, P. Maunz, P. W. H. Pinkse, and G. Rempe, *Phys. Rev. Lett.* **82**, 3791 (1999).
  - [25] K. Murr, *J. Phys. B* **36**, 2515 (2003).
  - [26] P. Meystre and M. Sargent III, *Elements of Quantum Optics* (Springer-Verlag, Berlin, 1999), 3rd ed.
  - [27] Q. A. Turchette, C. J. Hood, W. Lange, H. Mabuchi, and H. J. Kimble, *Phys. Rev. Lett.* **75**, 4710 (1995).
  - [28] Y. Shimizu *et al.*, *Phys. Rev. Lett.* **89**, 233001 (2002).